Research Square

Preprints are preliminary reports that have not undergone peer review.
They should not be considered conclusive, used to inform clinical practice,
or referenced by the media as validated information.

Shelf–Fjord Exchange Regulated by Recirculating Greenland Meltwater in Glacial Troughs

Jie Huang

jhuang@whoi.edu

Woods Hole Oceanographic Institution https://orcid.org/0000-0003-1134-5752

Robert Pickart

Woods Hole Oceanographic Institution https://orcid.org/0000-0002-7826-911X

Michael Spall

Woods Hole Oceanographic Institution

Paul Myers

University of Alberta https://orcid.org/0000-0003-4514-2654

Frank Bahr

Woods Hole Oceanographic Institution

Ben Kopec

Michigan Technological University

Emil Jeansson

https://orcid.org/0000-0002-2501-3479

Jeffrey Welker

University of Alaska Anchorage https://orcid.org/0000-0002-3865-4822

Article

Keywords:

Posted Date: August 18th, 2025

DOI: https://doi.org/10.21203/rs.3.rs-7321564/v1

License: This work is licensed under a Creative Commons Attribution 4.0 International License.
Read Full License

Additional Declarations: There is **NO** Competing Interest.

Version of Record: A version of this preprint was published at Nature Geoscience on November 25th, 2026. See the published version at https://doi.org/10.1038/s41561-026-02147-2.

Title: Shelf–Fjord Exchange Regulated by Recirculating Greenland Meltwater in Glacial Troughs

Authors: Jie Huang[1*], Robert S. Pickart[1], Michael A. Spall[1], Paul Myers[2], Frank Bahr[1], Ben Kopec[3], Emil Jeansson[4], and Jeffrey M. Welker[5,6,7]

Affiliations:

[1] Woods Hole Oceanographic Institution, Woods Hole, MA 02543, USA

[2] Department of Earth and Atmospheric Sciences, University of Alberta, Edmonton, AB T6G 2E3, Canada

[3] Great Lakes Research Center, Michigan Technological University, Houghton, MI 49931, USA

[4] NORCE Norwegian Research Centre, Bjerknes Centre for Climate Research, Bergen 5007, Norway

[5] University of Oulu, Oulu 90014, Finland

[6] University of Alaska Anchorage, Anchorage, Alaska 99508, USA

[7] University of the Arctic, Rovaniemi 96200, Finland

Submitted to *Nature Geoscience*

August 2025

*Corresponding author: jhuang@whoi.edu

Abstract

The Greenland Ice Sheet is rapidly losing mass due to climate warming, contributing significantly to global sea level rise and altering ocean circulation and ecosystems. Yet, the processes controlling interactions between glacial fjords and the adjacent continental shelf and slope are not fully understood, particularly the role of bathymetric troughs in modulating water exchange between the fjords and boundary current system. Here we present high-resolution shipboard, reanalysis, and numerical model data across several deep troughs in West Greenland, revealing a recurring anticyclonic recirculation of glacial meltwater within the inner Uummannaq trough, which isolates the glacial fjord from subsurface Atlantic Water inflow and thus limits oceanic heat penetration. This circulation—driven by seasonal meltwater discharge and modulated by wind forcing—contrasts with the adjacent Jakobshavn trough, where more efficient exchange prevents such retention. The presence of recirculating freshwater correlates with enhanced nutrient concentrations and isotopic signatures, suggesting broader biogeochemical impacts. Analogous recirculation patterns are also present in some East Greenland fjords where ice loss has been comparatively reduced. Our findings emphasize the critical role of fjord-shelf topography and regional dynamics in modulating Greenland's glacial melting, freshwater export, and nutrient delivery, highlighting the need for improved representation of these processes in climate models.

Main text

1. Introduction

The Greenland Ice Sheet is undergoing substantial and accelerating mass loss in response to ongoing climate warming[1,2]. This loss accounts for roughly one-quarter of the rate of global sea level rise[3] and has been implicated in altering regional and global ocean circulation patterns[4,5], including the Atlantic Meridional Overturning Circulation—a key component of Earth's climate system. In addition, enhanced meltwater discharge from Greenland is changing ocean stratification[6] and affecting marine ecosystems[7,8]. One of the most pronounced changes in Greenland's freshwater system is the intensification of meltwater export through glacial fjords[9,10], particularly along the west coast, where major glaciers such as Jakobshavn glacier have experienced remarkable retreat over recent decades[11,12]. These large marine-terminating glaciers have contributed more than half of the ice loss from Greenland since 2000[2]. While numerous studies have investigated the dynamics of these glaciers and the associated fjords[13-15], direct observations of interactions between the continental slope circulation and fjord circulation in this region remain sparse.

The boundary current system around Greenland transports both glacial meltwater and Arctic-origin freshwater as it flows along the continental slope and shelf[16-18] (Fig. 1). Beneath this surface Polar Water (PW) layer, resides the warm and salty subtropical-origin Atlantic Water (AW), which underwent a shift to warmer temperatures starting in the 1990s[19,20]. This warm water is present on the continental shelves adjacent to the fjords[18,21] and has been suggested to play an important role in controlling submarine melting of Greenland's glaciers[22,23]. One of the unique aspects of the bathymetry around Greenland are the deep, glacially carved troughs that cut into the shelf from

the continental slope and connect directly to the glacial fjords. These troughs, varying in depth, width, and orientation, potentially serve as efficient conduits for transporting the warm AW to the inner shelf. Previous studies, mostly in Antarctica, have identified mechanisms such as eddy activity[24], wind reversals[25], and breaking Rossby waves[26] which facilitate injections of warm water onshore via the troughs. However, around Greenland, lack of high-resolution measurements has hindered our understanding of the kinematic and dynamic linkages between the boundary current system and the fjord interiors[27]. The role of bathymetry, as well as the interplay between internal and external forcing, remains poorly understood[28]. Moreover, how these troughs modulate the spatial variability of freshwater outflow and how this outflow interacts with the subsurface warm water at varying timescales have not been fully explored[29].

To help address these gaps, a high-resolution shipboard survey was conducted from late summer to early fall of 2021, collecting detailed hydrographic, velocity, and biogeochemical data across multiple deep troughs connecting the West Greenland slope/shelf with glacial fjords. Using these observations, we characterize and contrast the water mass structure and circulation patterns in Uummannaq and Jakobshavn troughs. Further investigation using ocean reanalysis datasets and output from a 1/60° high-resolution ocean numerical model reveals a previously unrecognized regime leading to interaction between Greenland's outflowing discharge water and inflowing warm AW in deep troughs. The underlying dynamics of this regime and its implications for regulating the Greenland ice sheet melt and biogeochemical cycle are discussed.

2. Results

2.1. Hydrographic and velocity structure in the trough systems

During the 2021 survey, six high-resolution sections were sampled across three major troughs connecting the West Greenland shelf with glacial fjords (Fig. 1). The outer Uummannaq section (section U2) shows the expected hydrographic and velocity structure observed in such trough systems[14,21] (Fig. 2a). Three distinct water masses were identified: (1) a surface layer of warm and fresh Polar Water (warm PW), which is a mixture of Greenland discharge and Arctic-origin freshwater transported by the West Greenland Coastal Current; (2) a mid-depth layer of cold and relatively fresh Polar Water (cold PW); and (3) a deep layer of warm and salty AW, originating from the continental slope.

As demonstrated in previous studies[30,31], the flow along the coast of Greenland tends to be steered into the troughs along their upstream flanks and steered back offshore along their downstream flanks. Consistent with this, our velocity observations in the outer Uummannaq trough show inflow (towards the fjord) on the southern side and outflow on the northern side, corresponding to a doming of the pycnocline across the trough. Interestingly, a bottom intensified flow associated with AW was present in the deepest part of the trough. A similar structure of bottom-intensified AW flow was also observed along the west Greenland slope[21] in Baffin Bay, highlighting the trough's role as an a conduit for shelf-fjord exchange of this warm water.

Using the velocity measurements in conjunction with the hydrographic data, we quantify the volume transport of the different water masses through the three trough systems in potential temperature/salinity (θ/S) space, with red denoting net inflow toward the fjord and blue denoting

net outflow away from the trough (Fig. 2c). Across most sections, AW (potential density > 27.25 kg/m^3) consistently enters the fjords at depth through the troughs, with the exception of the inner Uummannaq section (section U1, explored in detail in Section 2.2). At Upernavik trough (section P), the inflowing transport of AW is relatively small, likely due to the weakening of the boundary current as it progresses farther northward into Baffin Bay[21]. Overall, while the surface-layer circulation in the trough systems is variable, the deep inflow of AW is more stable and persistent. The net transport of AW inflow for the four sections excluding U1 and P is 0.22±0.05 Sv (where the uncertainty is the standard error).

2.2. Recirculation of Greenland discharge water in the inner trough

As noted above, the inner Uummannaq section exhibited negligible bottom inflow of AW, even though this section was occupied only 5 hours after the outer Uummannaq section. In fact, there were substantial differences in the hydrographic and velocity structure throughout the two sections (compare Figs. 2a and 2b). As expected, the upper layer at the inner section was fresher than that at the outer section. Most notably, however, the inner section showed the opposite flow pattern, with outflow on the southern side of the trough and inflow on the northern side (also seen in Fig. 3a showing the shipboard ADCP velocity data). Furthermore, in contrast to the doming of the pycnocline at the outer section, the inner section was characterized by a bowling of the pycnocline across the trough.

To investigate the nature of this flow reversal, we firstly examined the Global Ocean Physics Analysis and Forecast (GOPA) reanalysis, which successfully reproduces the hydrographic and velocity structure observed in both the outer and inner Uummannaq sections during the time period

of the shipboard survey in 2021 (Supplementary Fig. 1). Interestingly, the GOPA reanalysis reveals the presence of an anticyclonic circulation corresponding to a surface freshwater anomaly in the inner part of the Uummannaq trough (Fig. 3b). This flow pattern and freshwater anomaly first appeared in mid-September 2021 in GOPA and persisted for roughly a month before it slowly propagated offshore. The transport associated with the feature was order 0.25–0.5 Sv, corresponding to a steady decline in the upper layer (0-50 m) averaged salinity in the inner trough by 0.05 over the month-long period (Fig. 3c). These results imply that the observed flow pattern was driven by the discharge of glacial water. Such a flow pattern was not found in other reanalysis products such as GLORYS12 and AMOR3D, likely due to their coarser temporal or spatial resolution. This emphasizes the need for high-resolution data to accurately capture the shelf-fjord exchange processes within complex trough systems.

In addition to GOPA, we analyzed output from a 1/60° high-resolution numerical model (see Methods Section for details). Although not contemporaneous with the cruise, the model offers enhanced spatial resolution, providing valuable insights into the mechanisms driving the observed flow reversal. Transport timeseries for the northern and southern portions of the inner Uummannaq section revealed five flow reversal events similar to the one observed during the 2021 shipboard survey over the 3.5-year period of the model simulation (Supplementary Fig. 2), with an average duration of 28±6 days per event (the uncertainty is the standard deviation). Notably, most of these events occurred from May to July during the period of seasonally increasing Greenland meltwater discharge (Fig. 4a). To further explore the dynamics behind these events, we constructed a composite of the five model flow reversals and documented the evolution of circulation and lateral freshwater distribution as a function of normalized time (Fig. 3d-i). Prior to the reversal, the typical

151 circulation was evident: inflow in the southern part of inner trough and outflow in the north. As
152 the reversal began, an anticyclonic circulation developed in the inner trough, accompanied by a
153 negative freshwater anomaly in the upper 50 m. The anticyclonic flow and freshwater signal
154 continued to intensify, then slowly propagated offshore at an average speed of ~2 km/day. These
155 findings suggest that such a recirculation of discharge water in the inner trough is relatively stable,
156 consistent with laboratory experiments showing eddies trapped in topographic troughs[32]. Similar
157 anticyclonic features have been documented at river mouths, attributed to the influence of Earth's
158 rotation on buoyant river runoff[33]. Our results indicate that glacial discharge may generate
159 analogous circulation features in fjord-trough systems, although a large amount of the freshwater
160 originates from the base of glaciers at depth before being uplifted[34].
161
162 Both the numerical model and GOPA reanalysis suggest that the anticyclonic circulation is a
163 dynamical response to the buoyant Greenland discharge. The low salinity water is less dense than
164 the ambient waters and so has a positive sea surface height anomaly. Through the related pressure
165 gradient, the surface flow is anticyclonic. This anticyclonic flow penetrates below the surface to
166 the AW but is smaller in magnitude because the hydrographic structure reduces the lateral pressure
167 gradient with depth. This aligns with the finding that most of the events occurred during the
168 melting season. That said, there were two events that took place after the melting season in late-
169 summer/early-fall (events M5 and G1 in Fig. 4a). Analysis of the wind forcing during these two
170 events revealed a transition from downwelling- to upwelling-favorable winds (see Supplementary
171 Fig. 3 for the G1 event). During the melt season, downwelling-favorable winds generally suppress
172 the offshore export of freshwater[35,36]. As the wind regime shifts, the accumulated freshwater can
173 thus be released, initiating the dynamically driven recirculation of the discharge water. This

174 demonstrates that wind forcing can play a role in modulating retention and release to the trough,
175 thereby influencing the occurrence and timing of such flow reversals.
176
177 **2.3. Impact on Greenland ice sheet melt and the biogeochemical cycle**
178 Our shipboard observations, the GOPA reanalysis data, and the 1/60° high-resolution model output
179 together reveal a distinct regime for the fate of glacial discharge in the Uummannaq trough.
180 Freshwater discharge accumulates in the inner trough due to the establishment of an anticyclonic
181 gyre that then slowly propagates offshore. In the inner Uummannaq section, this accumulation
182 constricts the AW layer at depth, thereby limiting heat transport from the slope and shelf regions
183 into the glacial fjords. This mechanism aligns with satellite altimetry observations[12], which show
184 comparatively smaller changes in ice surface elevation in the Uummannaq region relative to those
185 elsewhere in northwestern Greenland (Fig. 5a).
186
187 In contrast, the Jakobshavn trough exhibits no evidence of a similar flow reversal or gyre formation,
188 despite receiving more than twice the volume of freshwater discharge due to the rapid retreat of
189 Jakobshavn glacier (Fig. 4a). This discrepancy is likely due to differences in bathymetry: the inner
190 Jakobshavn region has a deep channel north of Disko Island (Fig. 4b) and a broad southern opening,
191 which facilitate more efficient exchange between the boundary current system and fjord freshwater.
192 Additionally, the northward-flowing West Greenland Coastal Current—characterized by relatively
193 warm, saline water—reaches Jakobshavn before Uummannaq, likely exerting a stronger advective
194 influence at the southern location. This interpretation is supported by historical hydrographic data,
195 which show higher surface salinities in the inner Jakobshavn area compared to Uummannaq (Fig.
196 4b).

Basal meltwater from glaciers has been suggested as an important source of nutrients to Greenland's shelf and slope regions, influencing primary production and biogeochemical cycling in the high-latitude ocean[7,37,38]. Nutrient data collected during the 2021 survey reveal elevated concentrations of nitrate, phosphate, and silicate at depth (potential density > 27.25 kg/m^3) in the Uummannaq inner trough relative to the outer trough (Fig. 4c). In fact, the values in Uummannaq trough as a whole were the highest of any trough surveyed during the cruise. This nutrient enrichment likely results from the trapping and prolonged residence time of basal meltwater entrained into the AW layer, even though overall meltwater input from Uummannaq glaciers is lower than that from Jakobshavn. Consistent with the nutrient distributions at depth, lower oxygen isotope ($\delta^{18}O$) concentrations and higher deuterium excess values in the PW from isotope measurements also indicate higher meltwater fractions in the upper water column of inner Uummannaq Trough versus Jakobshavn[39] (Fig. 4c). Recent work focusing on a southern Greenland trough (Narsaq) demonstrated that signals of meltwater may be masked by rapid vertical mixing or dilution through exchange with water in the coastal current[28]. These processes may help explain the lower observed nutrient concentrations and deuterium excess values in the Jakobshavn area which is more strongly influenced by the West Greenland Coastal Current than the Uummannaq area farther north.

3. Discussion

The Uummannaq and Jakobshavn troughs exhibit distinct dynamics in the shelf-fjord exchange of water masses, nutrients, and isotopic tracers. These differences demonstrate the variability in shelf-fjord interactions around Greenland, where trough systems differ in size, orientation, and

bathymetric structure. The GOPA reanalysis reveals that anticyclonic-like recirculation of meltwater is a recurring feature in several troughs along East Greenland (Fig. 5b-c). These regions also correspond to areas that have experienced minimal ice height changes in recent years, suggesting that such recirculation may act to insulate outlet glaciers by limiting the penetration of warm Atlantic Water into fjords. This finding reinforces the critical role of localized circulation in modulating glacier-ocean heat exchange and ice sheet mass balance. Future analyses are needed to systematically assess this role relative to other mechanisms such as atmospheric warming[23,40] and geological conditions[41,42]. Our results emphasize the need to better integrate detailed fjord dynamics with the larger-scale ocean circulation in both observations and models. Bridging this gap in scale is essential for improving projections of Greenland Ice Sheet evolution and understanding its broader influence on oceanographic and biogeochemical systems in the high-latitude North Atlantic.

4. Methods

4.1. Shipboard data.

The hydrographic, velocity, nutrient, and oxygen isotope data used this study were collected aboard the US Coast Guard Cutter (USCGC) *Healy* between 17 September and 4 October 2021. The vessel was equipped with a Sea-Bird 911+ conductivity-temperature-depth (CTD) rosette system with 24 Niskin bottles for seawater sampling. Ocean velocity was measured using a shipboard acoustic Doppler current profiler (ADCP). See Huang et al. (2024)[21] for details regarding data collection and processing as well as measurement accuracy. The survey sampled three major troughs on the West Greenland shelf, with a station spacing of 5–10 km (see Fig. 1 for locations), including two sections across the Uummannaq trough, three across the Jakobshavn

trough, and one across Upernavik trough. Absolute geostrophic velocities were calculated by referencing the thermal wind shear derived from CTD profiles to the observed ADCP velocities, following methods detailed in Huang et al. (2021)[43]. Vertical sections of potential temperature (referenced to the sea surface), practical salinity, potential density (referenced to sea surface), and absolute geostrophic velocity were constructed using Laplacian-spline interpolation[44].

4.2. Historical hydrographic data

The historical hydrographic data were compiled from numerous sources, including the Unified Database for Arctic and Subarctic Hydrography (UDASH)[45], Amundsen Science data collection, Davis Strait cruises, World Ocean Database (WOD)[46], and the Oceans Melting Greenland (OMG) program[47]. Datasets were merged into a single composite archive, with duplicates removed. Quality control procedures applied by the original data providers were retained. See Supplementary Fig. 4 for the spatial and temporal data coverage in the Uummannaq and Jakobshavn areas. Access information for each data source is provided in the Data Availability Section.

4.3. GOPA reanalysis

The Global Ocean Physics Analysis and Forecast (GOPA) product, available from the Copernicus Marine Environment Monitoring Service (CMEMS), provides 3D fields of potential temperature, salinity, and ocean currents on a 1/12° horizontal grid and 50 vertical levels. GOPA is based on the NEMO ocean model and initialized from the global ocean reanalysis in October 2016. It assimilates along-track satellite altimetry, sea surface temperature, sea ice concentration, and in-situ temperature and salinity profiles. Compared to GLORYS12, GOPA offers higher temporal

resolution, with outputs available at 1-hour, 6-hour, daily, and monthly intervals through a two-year rolling archive. The 6-hour data were used in this study.

4.4. 1/60 high-resolution model output

Output from a high-resolution (1/60°) configuration of the NEMO ocean model[48] coupled with the LIM2 sea ice model[49], spanning 1993–1997, was used. This limited time period reflects the computational cost of such a very high-resolution configuration, which is in the process of being extended to the present. The model domain includes Baffin Bay, the Labrador Sea, and covers the Arctic Ocean to Bering Strait. Grid spacing in Baffin Bay is <1 km, which is sufficient to resolve the baroclinic Rossby radius of deformation (~10 km, estimated using the *Healy* data) and topographic troughs extending from the shelfbreak into the fjords. The model includes 50 vertical levels, with resolution ranging from 1 m at the surface to 453 m at 5728 m depth.

Tidal forcing includes the nine primary constituents from the TPXO9.v3 atlas. Greenland Ice Sheet meltwater discharge is applied as a boundary condition, based on Bamber et al. (2018)[50]. Icebergs are parameterized, and river runoff is specified using the HYPE hydrological model[51]. Bottom topography is from the GEBCO 1/60° bathymetric dataset. The model is initialized using GLORYS12 fields and driven by hourly ERA5 atmospheric forcing.

4.5. ERA5 atmosphere forcing data

10-m winds are from the ECMWF ERA5 reanalysis, with 0.25° horizontal resolution and hourly temporal resolution. Previous studies have demonstrated favorable agreement between observations and Integrated Forecast System (IFS)-based reanalysis products around Greenland[52].

4.6. Greenland discharge data

Solid ice and liquid water discharge data from the Greenland Ice Sheet were obtained from Mankoff et al. (2020a, b)[53,54]. Ice discharge was estimated using observed ice velocity, thickness, and density at marine-terminating glaciers. Liquid freshwater discharge was derived from a regional climate model, incorporating melt runoff, precipitation, refreezing, and land runoff components. For methodology and uncertainty quantification, see Mankoff et al. (2020a, b)[53,54]. These datasets are widely used to represent freshwater forcing from the Greenland Ice Sheet. We used the daily discharge timeseries from 1990 to 2021.

5. Acknowledgements

We thank Commanding Officer Kenneth Boda and the crew of the USCGC *Healy* for their expertise and dedication in obtaining the shipboard measurements through collaboration with the science party. Funding was provided by the U. S. National Science Foundation Office of Polar Programs under grants OPP-2034801 and OPP-2211691 (J. Huang, R. Pickart, and M. Spall), and OPP-2133156 (J. Welker and B. Kopec). The isotope measurements were supported by J. Welker's UArctic Research Chairmanship. The ARC60 model experiment was developed under funding from a Natural Sciences and Engineering Research Council of Canada (NSERC) grant awarded to P. Myers (Grant RGPIN-2020-04344), as well as computational resources provided by the Digital Research Alliance of Canada (alliancecan.ca).

6. Data Availability

1. The data from the *Healy* survey in 2021 are available at DOI: https://arcticdata.io/catalog/view/doi:10.18739/A2DB7VR5M.

2. Historical hydrographic data are available at each individual source: UDSASH (https://doi.pangaea.de/10.1594/PANGAEA.872931), Amundsen Science data collection (https://amundsenscience.com/data/data-access/), Davis Strait cruises (https://arcticdata.io/catalog/portals/DSOS/Data), World Ocean Database (https://www.ncei.noaa.gov/products/world-ocean-database), and Oceans Melting Greenland program (https://podaac.jpl.nasa.gov/dataset/OMG_L1_FLOAT_ALAMO).

3. The data from GOPA reanalysis are available at: https://data.marine.copernicus.eu/product/GLOBAL_ANALYSISFORECAST_PHY_001_024/description.

4. The ERA5 wind data are available at: https://www.ecmwf.int/en/forecasts/datasets/reanalysis-datasets/era5.

5. The 1/60° high-resolution model output data are available from the authors upon request.

6. The Greenland discharge data are available at: https://dataverse.geus.dk/dataverse/ice_discharge; https://dataverse.geus.dk/dataverse/freshwater.

7. References

1 Van den Broeke, M. *et al.* Partitioning recent Greenland mass loss. *science* **326**, 984-986 (2009).

2 Enderlin, E. M. *et al.* An improved mass budget for the Greenland ice sheet. *Geophysical Research Letters* **41**, 866-872 (2014).

3 Church, J. A. *et al.* Revisiting the Earth's sea-level and energy budgets from 1961 to 2008. *Geophysical Research Letters* **38** (2011).

4 Lazier, J. R. Oceanographic conditions at ocean weather ship Bravo, 1964–1974. *Atmosphere-ocean* **18**, 227-238 (1980).

5 Swingedouw, D. *et al.* AMOC recent and future trends: A crucial role for oceanic resolution and Greenland melting? *Frontiers in Climate* **4**, 838310 (2022).

6 Bamber, J., Van Den Broeke, M., Ettema, J., Lenaerts, J. & Rignot, E. Recent large increases in freshwater fluxes from Greenland into the North Atlantic. *Geophysical Research Letters* **39** (2012).

7 Arrigo, K. R. *et al.* Melting glaciers stimulate large summer phytoplankton blooms in southwest Greenland waters. *Geophysical Research Letters* **44**, 6278-6285 (2017).

8 Mortensen, J. *et al.* Subglacial discharge and its down-fjord transformation in West Greenland fjords with an ice mélange. *Journal of Geophysical Research: Oceans* **125**, e2020JC016301 (2020).

9 Rignot, E., Box, J., Burgess, E. & Hanna, E. Mass balance of the Greenland ice sheet from 1958 to 2007. *Geophysical Research Letters* **35** (2008).

10 Dukhovskoy, D. S. *et al.* Greenland freshwater pathways in the sub-A rctic S eas from model experiments with passive tracers. *Journal of Geophysical Research: Oceans* **121**, 877-907 (2016).

11 Joughin, I., Abdalati, W. & Fahnestock, M. Large fluctuations in speed on Greenland's Jakobshavn Isbrae glacier. *Nature* **432**, 608-610 (2004).

12 Slater, T. *et al.* Increased variability in Greenland Ice Sheet runoff from satellite observations. *Nature Communications* **12**, 6069 (2021).

13 Sutherland, D. A., Straneo, F. & Pickart, R. S. Characteristics and dynamics of two major Greenland glacial fjords. *Journal of Geophysical Research: Oceans* **119**, 3767-3791 (2014).

14 Straneo, F. & Cenedese, C. The dynamics of Greenland's glacial fjords and their role in climate. *Annual review of marine science* **7**, 89-112 (2015).

15 Khazendar, A. *et al.* Interruption of two decades of Jakobshavn Isbrae acceleration and thinning as regional ocean cools. *Nature Geoscience* **12**, 277-283 (2019).

16 Gillard, L. C., Hu, X., Myers, P. G. & Bamber, J. L. Meltwater pathways from marine terminating glaciers of the Greenland ice sheet. *Geophysical Research Letters* **43**, 10,873-810,882 (2016).

17 Foukal, N. P., Gelderloos, R. & Pickart, R. S. A continuous pathway for fresh water along the East Greenland shelf. *Science advances* **6**, eabc4254 (2020).

18 Rysgaard, S. *et al.* An updated view on water masses on the pan-west Greenland continental shelf and their link to proglacial fjords. *Journal of Geophysical Research: Oceans* **125**, e2019JC015564 (2020).

19 Holland, D. M., Thomas, R. H., De Young, B., Ribergaard, M. H. & Lyberth, B. Acceleration of Jakobshavn Isbræ triggered by warm subsurface ocean waters. *Nature geoscience* **1**, 659-664 (2008).

20 Rykova, T., Straneo, F. & Bower, A. S. Seasonal and interannual variability of the W est G reenland C urrent S ystem in the L abrador S ea in 1993–2008. *Journal of Geophysical Research: Oceans* **120**, 1318-1332 (2015).

21 Huang, J. *et al.* Water mass evolution and general circulation of Baffin Bay: Observations from two shipboard surveys in 2021. *Progress in Oceanography* **229**, 103322 (2024).

22 Straneo, F. & Heimbach, P. North Atlantic warming and the retreat of Greenland's outlet glaciers. *Nature* **504**, 36-43 (2013).

23 Slater, D. & Straneo, F. Submarine melting of glaciers in Greenland amplified by atmospheric warming. *Nature Geoscience* **15**, 794-799 (2022).

24 Brearley, J. A., Moffat, C., Venables, H. J., Meredith, M. P. & Dinniman, M. S. The role of eddies and topography in the export of shelf waters from the West Antarctic Peninsula shelf. *Journal of Geophysical Research: Oceans* **124**, 7718-7742 (2019).

25 Snow, T. *et al.* Alongshore winds force warm Atlantic water toward Helheim glacier in southeast Greenland. *Journal of Geophysical Research: Oceans* **128**, e2023JC019953 (2023).

26 St-Laurent, P., Klinck, J. M. & Dinniman, M. S. On the role of coastal troughs in the circulation of warm Circumpolar Deep Water on Antarctic shelves. *Journal of Physical Oceanography* **43**, 51-64 (2013).

27 Straneo, F. *et al.* The case for a sustained Greenland Ice Sheet-ocean observing system (GrIOOS). *Frontiers in Marine Science* **6**, 138 (2019).

28 Nelson, M. *et al.* Observations of water mass modification and cross-shelf exchange at Narsaq Trough, Greenland. *Journal of Geophysical Research: Oceans* **130**, e2024JC022246 (2025).

29 Gillard, L. C., Hu, X., Myers, P. G., Ribergaard, M. H. & Lee, C. M. Drivers for Atlantic-origin waters abutting Greenland. *The Cryosphere* **14**, 2729-2753 (2020).

30 Spurgin, J. M. & Allen, S. Flow dynamics around downwelling submarine canyons. *Ocean science* **10**, 799-819 (2014).

31 Sutherland, D. A. & Cenedese, C. Laboratory experiments on the interaction of a buoyant coastal current with a canyon: Application to the East Greenland Current. *Journal of physical oceanography* **39**, 1258-1271 (2009).

32 Wolfe, C. L. & Cenedese, C. Laboratory experiments on eddy generation by a buoyant coastal current flowing over variable bathymetry. *Journal of Physical Oceanography* **36**, 395-411 (2006).

33 Fujiwara, T., Sanford, L., Nakatsuji, K. & Sugiyama, Y. Anti-cyclonic circulation driven by the estuarine circulation in a gulf type ROFI. *Journal of Marine Systems* **12**, 83-99 (1997).

34 Karlsson, N. B. *et al.* A first constraint on basal melt-water production of the Greenland ice sheet. *Nature Communications* **12**, 3461 (2021).

35 Jackson, R. H., Straneo, F. & Sutherland, D. A. Externally forced fluctuations in ocean temperature at Greenland glaciers in non-summer months. *Nature Geoscience* **7**, 503-508 (2014).

36 Jackson, R. H., Lentz, S. J. & Straneo, F. The dynamics of shelf forcing in Greenlandic fjords. *Journal of Physical Oceanography* **48**, 2799-2827 (2018).

37 Hopwood, M. J. *et al.* How does glacier discharge affect marine biogeochemistry and primary production in the Arctic? *The Cryosphere* **14**, 1347-1383 (2020).

38 Croghan, D. *et al.* Western Greenland ice sheet-land-ocean interactions: Near-shore dissolved organic carbon 14C ages and composition in eastern Baffin Bay. *Journal of Geophysical Research: Biogeosciences* **130**, e2024JG008705 (2025).

39 Kopec, B. G. *et al.* Arctic freshwater sources and ocean mixing relationships revealed with seawater isotopic tracing. *Journal of Geophysical Research: Oceans* **129**, e2023JC020583 (2024).

40 Kanzow, T. *et al.* The system of atmosphere, land, ice and ocean in the region near the 79N Glacier in northeast Greenland: synthesis and key findings from the Greenland Ice Sheet–Ocean Interaction (GROCE) experiment. *The Cryosphere* **19**, 1789-1824 (2025).

41 Ran, J. *et al.* Vertical bedrock shifts reveal summer water storage in Greenland ice sheet. *Nature* **635**, 108-113 (2024).

42 Bevis, M. *et al.* Bedrock displacements in Greenland manifest ice mass variations, climate cycles and climate change. *Proceedings of the National Academy of Sciences* **109**, 11944-11948 (2012).

43 Huang, J., Pickart, R. S., Bahr, F., McRaven, L. T. & Xu, F. Wintertime water mass transformation in the western Iceland and Greenland Seas. *Journal of Geophysical Research: Oceans* **126**, e2020JC016893 (2021).

44 Smith, W. H. & Wessel, P. Gridding with continuous curvature splines in tension. *Geophysics* **55**, 293-305 (1990).

45 Behrendt, A., Sumata, H., Rabe, B. & Schauer, U. (2018).

46 Mishonov, A. V. *et al.* World Ocean Database 2023. (2024).

47 Fenty, I. *et al.* Oceans Melting Greenland: Early results from NASA's ocean-ice mission in Greenland. *Oceanography* **29**, 72-83 (2016).

48 Madec, G. NEMO ocean engine. (2015).

49 Fichefet, T. & Maqueda, M. M. Sensitivity of a global sea ice model to the treatment of ice thermodynamics and dynamics. *Journal of Geophysical Research: Oceans* **102**, 12609-12646 (1997).

50 Bamber, J. *et al.* Land ice freshwater budget of the Arctic and North Atlantic Oceans: 1. Data, methods, and results. *Journal of Geophysical Research: Oceans* **123**, 1827-1837 (2018).

51 Stadnyk, T. A. *et al.* Changing freshwater contributions to the Arctic: A 90-year trend analysis (1981–2070). *Elem Sci Anth* **9**, 00098 (2021).

52 Renfrew, I. A. *et al.* A comparison of aircraft-based surface-layer observations over Denmark Strait and the Irminger Sea with meteorological analyses and QuikSCAT winds. *Quarterly Journal of the Royal Meteorological Society: A journal of the atmospheric sciences, applied meteorology and physical oceanography* **135**, 2046-2066 (2009).

53 Mankoff, K. D. *et al.* Greenland liquid water discharge from 1958 through 2019. *Earth System Science Data* **12**, 2811-2841 (2020).

54 Mankoff, K. D. *et al.* Greenland Ice Sheet solid ice discharge from 1986 through March 2020. *Earth System Science Data* **12**, 1367-1383 (2020).

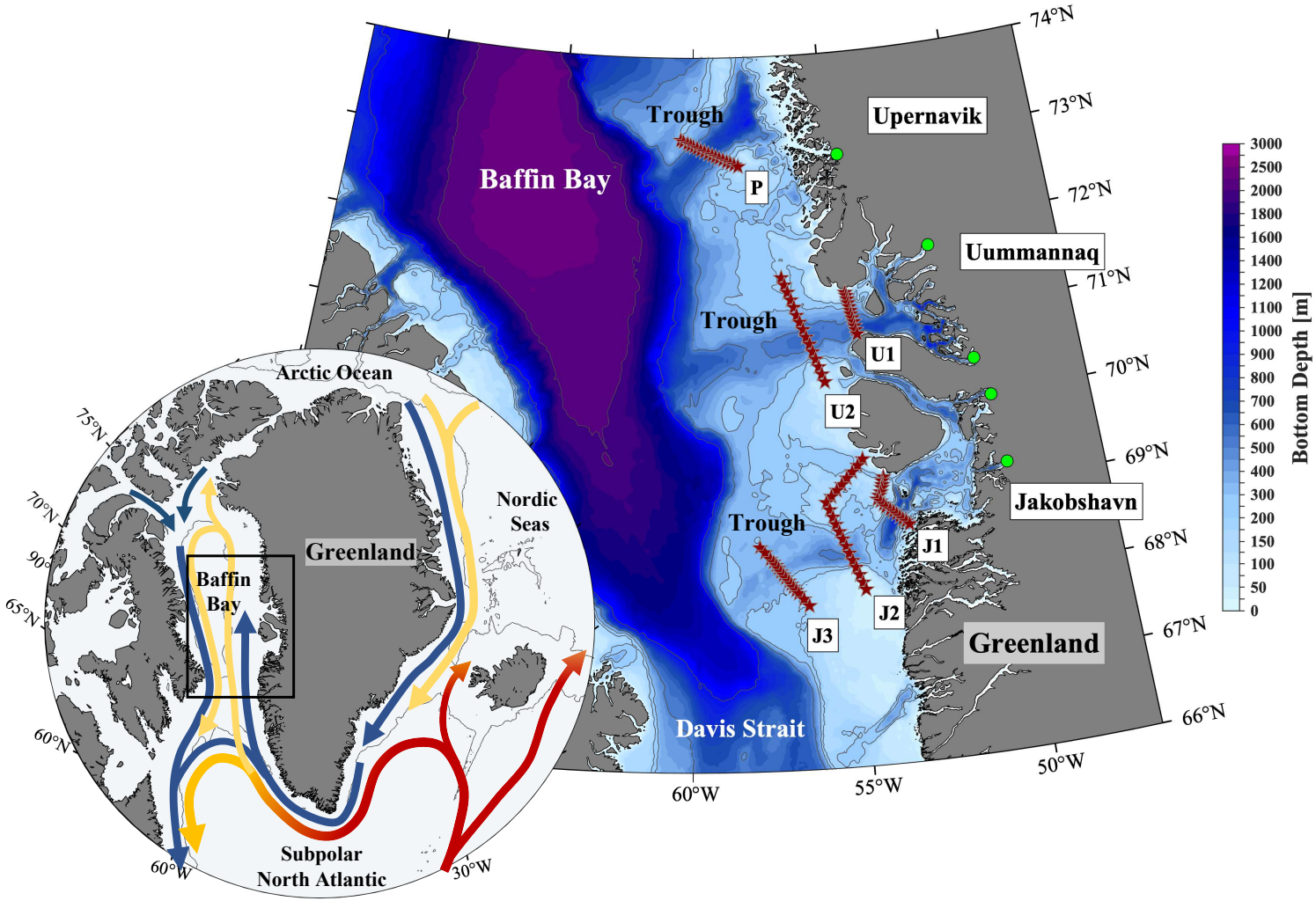


Figure 1. Schematic circulation and observation locations. (left) Schematic circulation of warm, salty Atlantic Water (red to yellow) and cold, fresh Polar Water (blue) around Greenland. The region shown in the right panel is outlined by the black box. (right) Stations (red stars) occupied on the West Greenland shelf during the 2021 Baffin Bay survey, including three transects across Jakobshavn trough (J1, J2, J3), two transects across Uummannaq trough (U1, U2), and one transect across Upernavik trough (P). Locations of major glaciers are marked by green dots. Bathymetry (color scale and gray contours) is from ETOPO1.

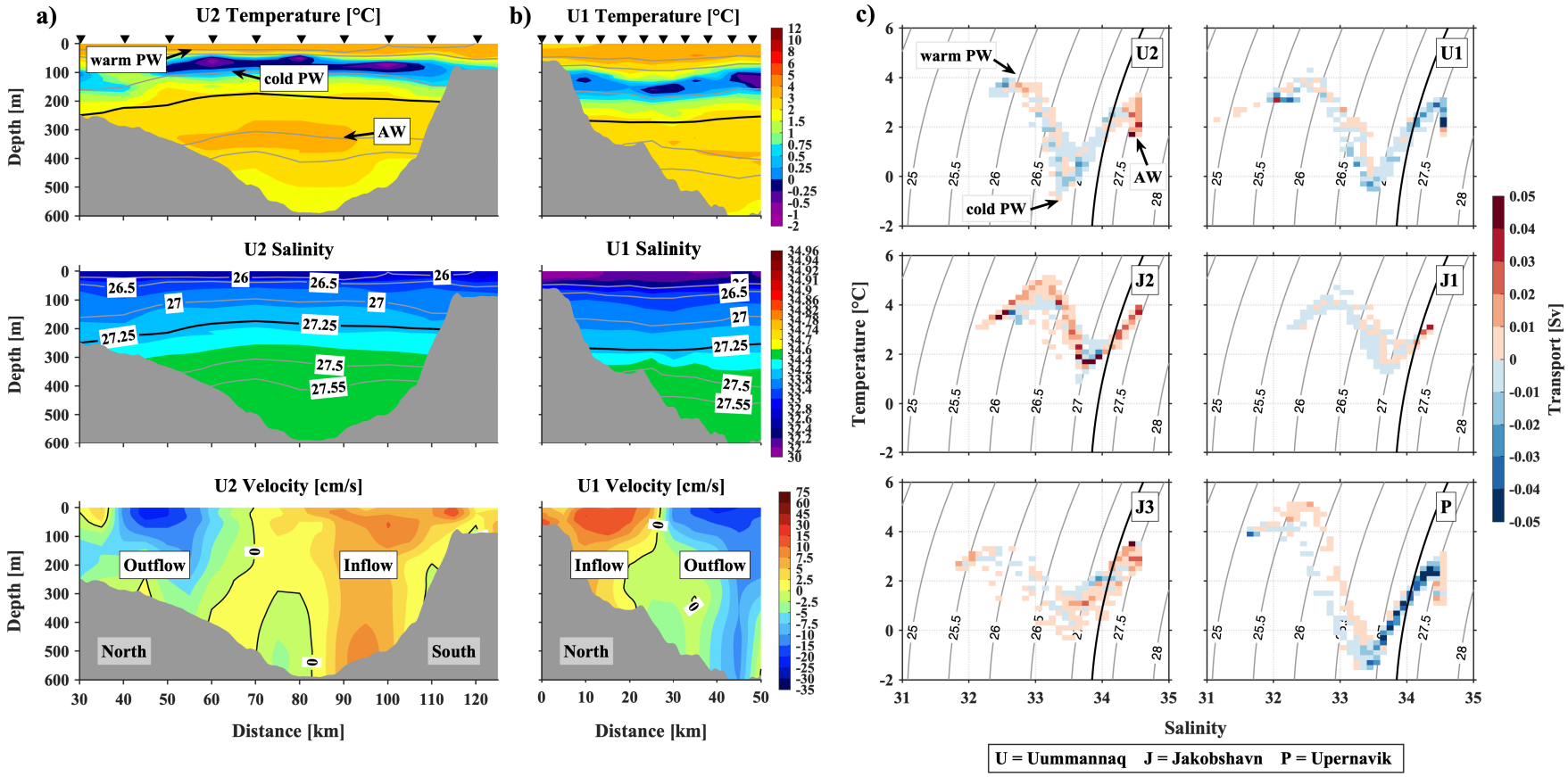


Figure 2. Hydrography, velocity, and volume transport in the trough systems. (a) Vertical sections of potential temperature (top), salinity (middle), and absolute geostrophic velocity (bottom) for the outer Uummannaq section (U2). Three characteristic water masses are identified: warm PW=warm Polar Water; cold PW=cold Polar Water; AW=Atlantic Water. Gray contours in the temperature and salinity panels indicate potential density (kg/m^3), with the 27.25 kg/m^3 isopycnal marking the top of the AW layer highlighted in black. In the velocity panel, black contours denote zero velocity; positive velocities are directed toward the glacial fjords. (b) Same as (a) but for the inner Uummannaq section (U1). (c) Volume transport through each trough section occupied during the 2021 survey, shown as a function of temperature and salinity. Positive values indicate transport toward the glacial fjords. Gray contours indicate density, with the 27.25 kg/m^3 isopycnal highlighted in black. See Figure 1 for the locations of each section.

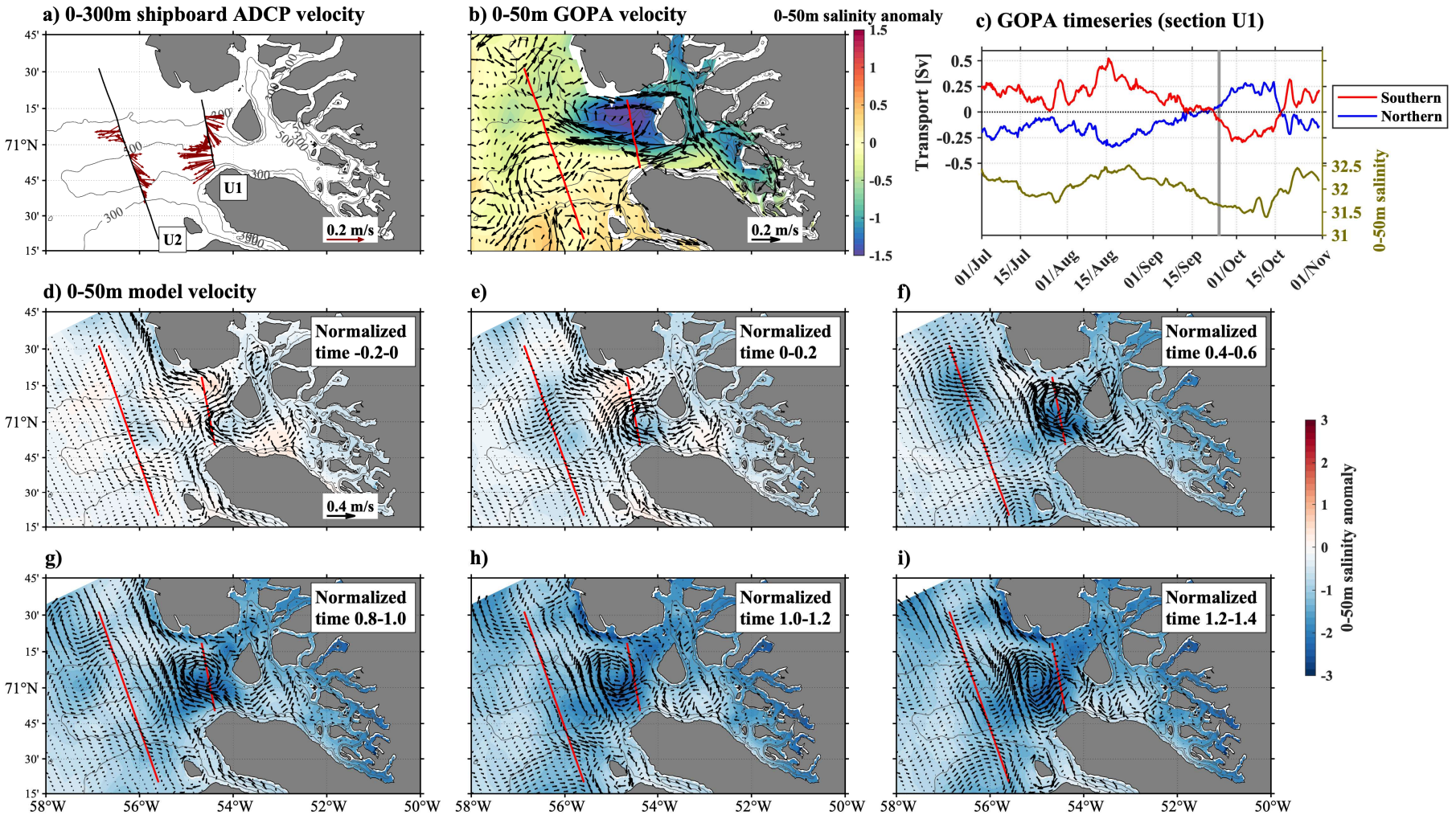


Figure 3. Flow reversal and recirculation of discharge water in Uummannaq. (a) Shipboard ADCP velocity averaged over 0-300 m during the 2021 survey. Black lines indicate the locations of the outer and inner Uummannaq sections. Bathymetry (gray contours) is from ETOPO1. (b) 0-50 m averaged velocity (vectors) and salinity anomaly (color) for the same period from the GOPA reanalysis. Red lines indicate the locations of the outer and inner Uummannaq sections. The salinity anomaly is computed by removing the mean salinity for the entire domain. (c) Timeseries of depth-integrated volume transport and upper 50 m averaged salinity for the inner Uummannaq

section (U1). Red and blue lines represent transport in the southern and northern halves of the section, respectively. The gray bar indicates the period of the cruise (the inner section was occupied on September 24, 2021). Positive transport values indicate flow toward the glacial fjords. (d-i) Composite 0-50 m averaged velocity (vectors) and salinity anomaly (color) for five flow reversal events identified in the high-resolution model output, shown at normalized time intervals: -0.2−0, 0−0.2, 0.4−0.6, 0.8−1.0, 1.0−1.2, and 1.2−1.4. Salinity anomalies are computed relative to the pre-reversal background (averaged over -0.4 to -0.2 normalized time).

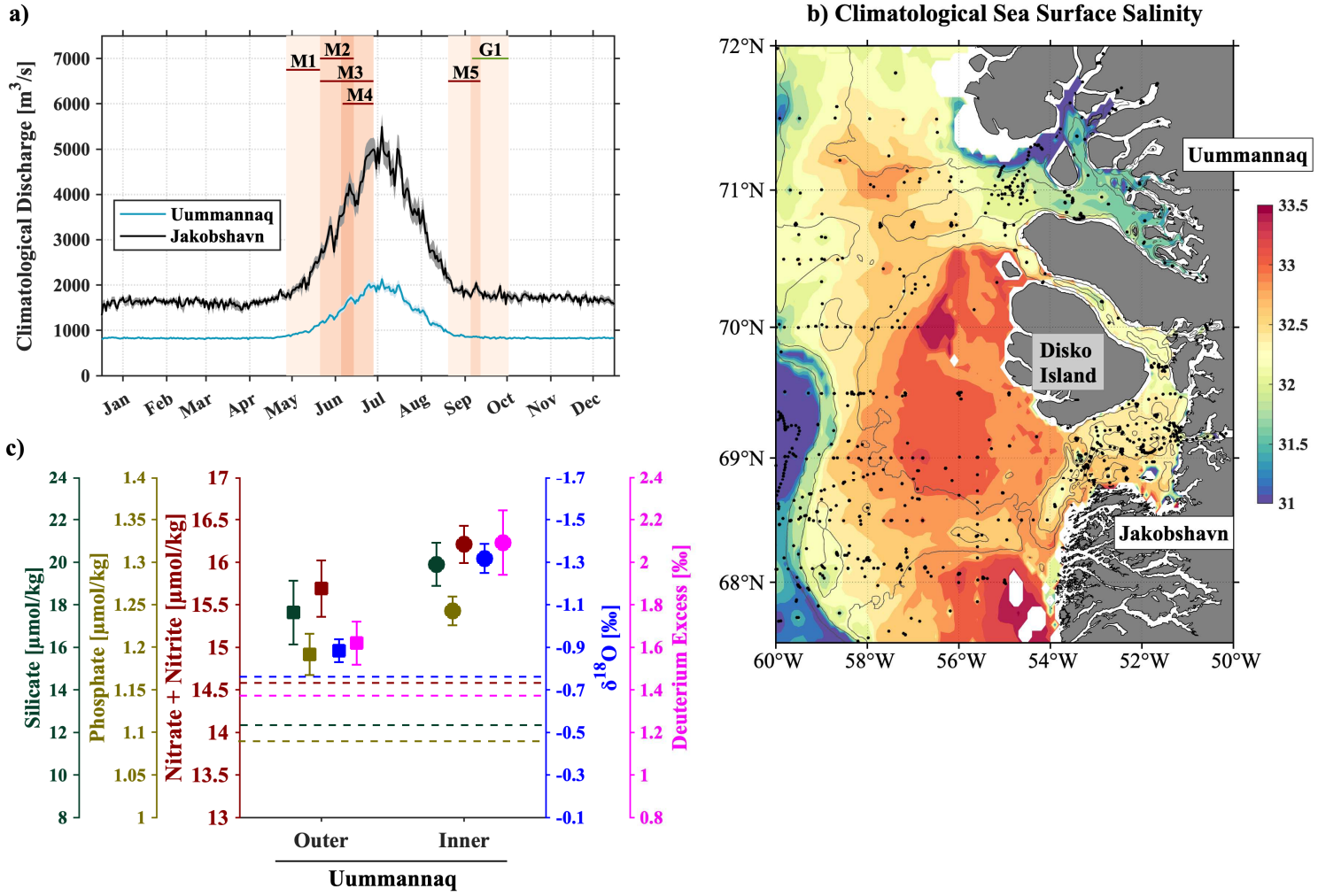


Figure 4. Contrasting discharge and water properties between Uummannaq and Jakobshavn. (a) Climatological seasonal cycle of total freshwater discharge (liquid and solid) for the Uummannaq (blue) and Jakobshavn (black) regions, using data from major sources between 1990-2021 (sources with liquid ice runoff > 20 m^3/s, liquid land runoff > 5 m^3/s, and ice discharge > 100 m^3/s). Orange shading denotes the timing of flow reversal events identified in the model output (events M1-M5) and the GOPA reanalysis (event G1, which

corresponded to the 2021 shipboard observations). The darker color indicates overlapping time periods. (b) Climatological near surface (upper 10 m) salinity derived from historical hydrographic data. Black dots mark the locations of the hydrographic profiles. Bathymetry (gray contours) is from ETOPO1. (c) Nutrient and isotope concentrations sampled in the Uummannaq (symbols, with outer (U2) and inner (U1) sections distinguished) and Jakobshavn troughs (dashed lines, mean of sections J1, J2, and J3). Nitrate + nitrite, phosphate, and silicate concentrations are for the AW (potential density > 27.25 kg/m^3). Oxygen isotope ($\delta^{18}O$) and deuterium excess values are for the PW (potential density ≤ 27.25 kg/m^3). Lower $\delta^{18}O$ (higher deuterium excess) values indicate a greater fraction of meltwater[39]. Error bars denote the standard error.

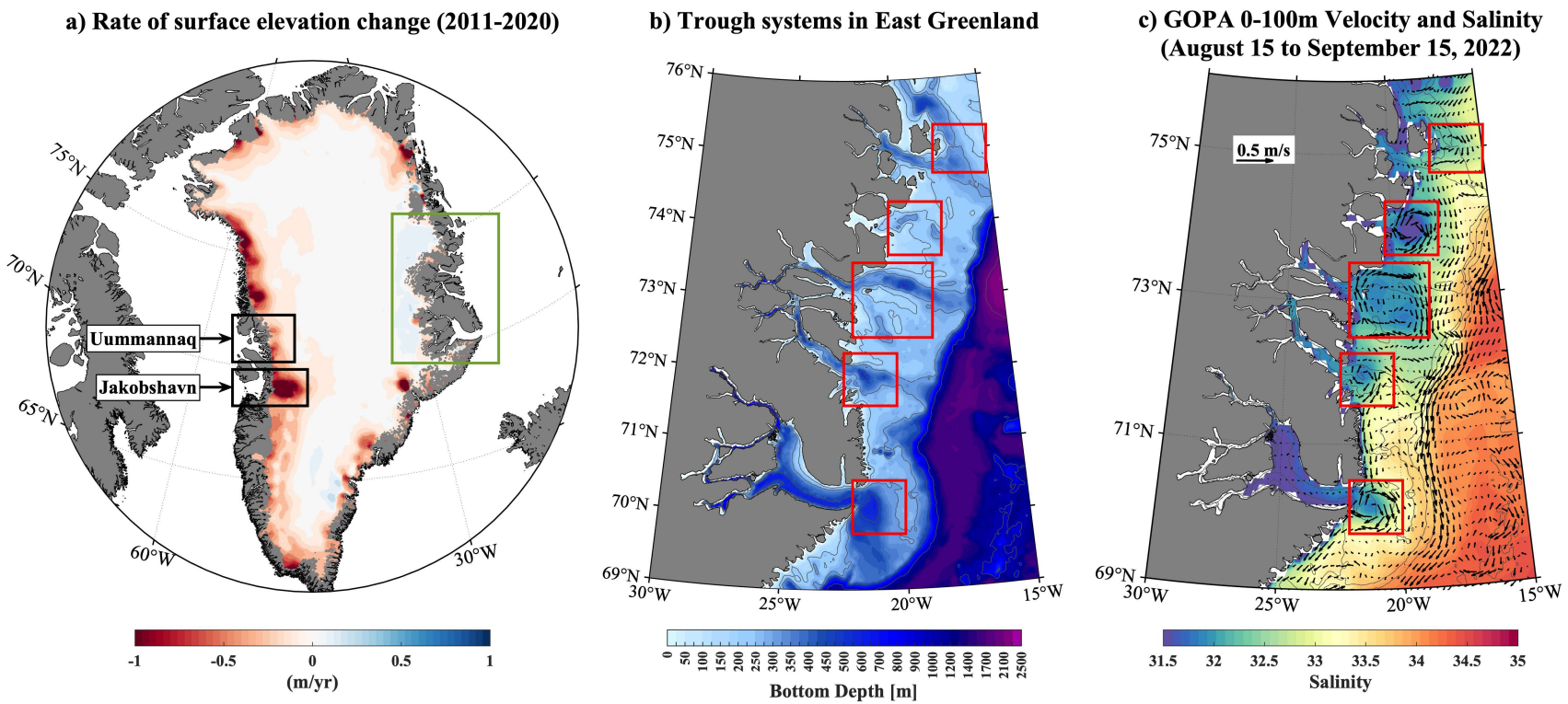
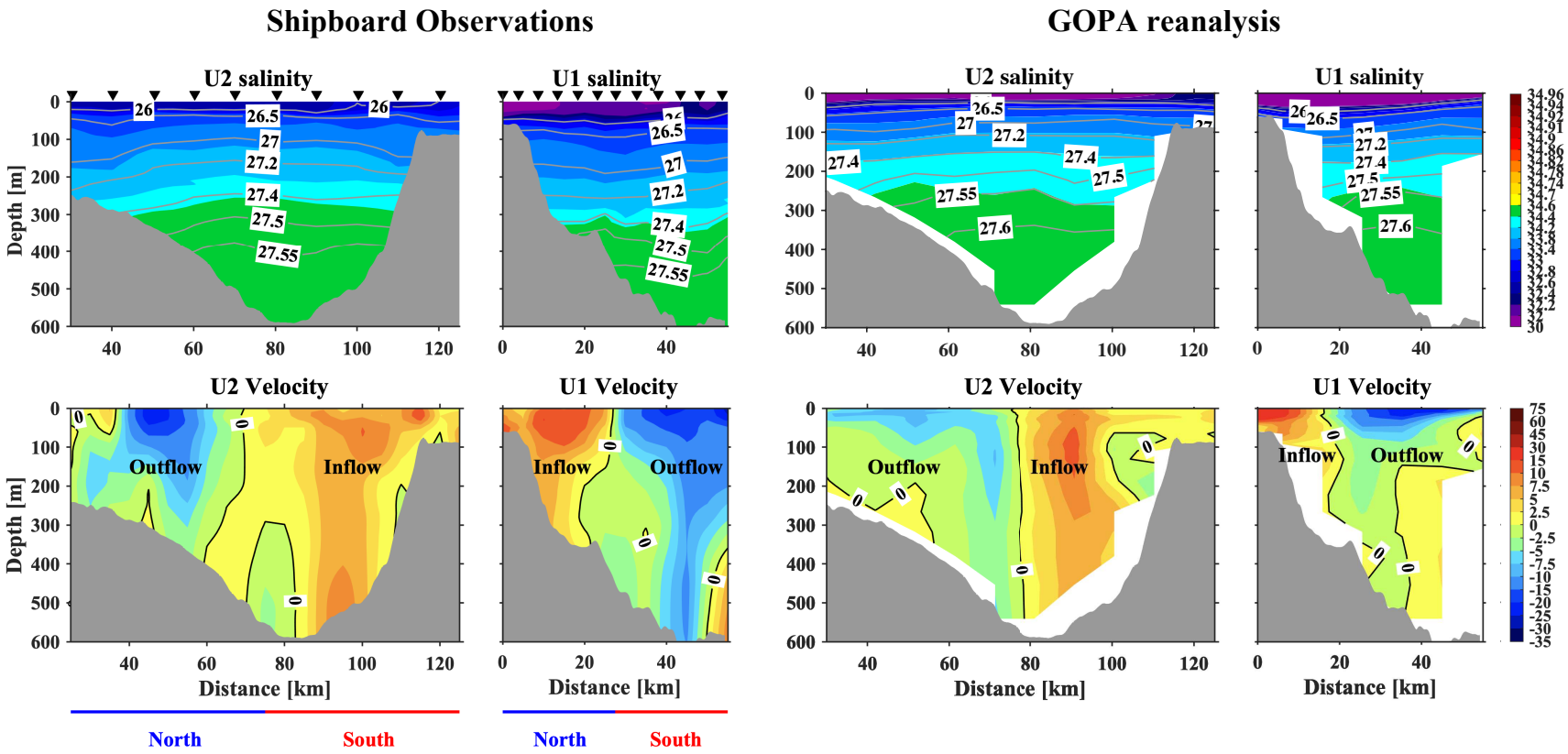
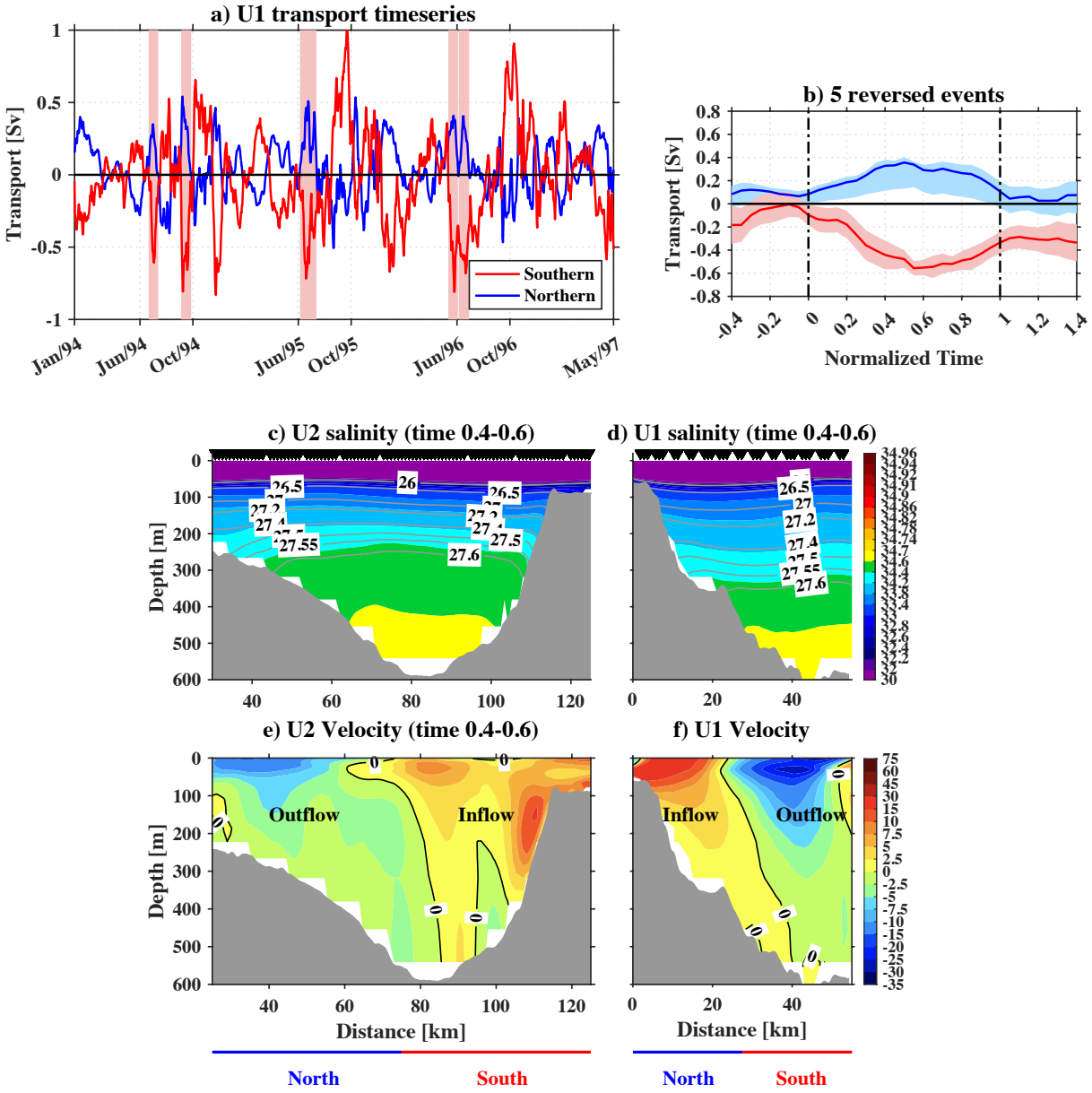


Figure 5. Trough systems in West/East Greenland. (a) Rate of Greenland surface elevation change between 2011 and 2020, based on data from Slater et al. (2021)[12]. The Uummannaq and Jakobshavn regions are outlined in black. The region of minimum reduction of surface elevation in East Greenland is outlined in green. (b) Bathymetry of the outlined domain in East Greenland in (a), with red boxes indicating inner trough regions. (c) Mean velocity and salinity in the upper 100 m averaged over the period 15 August to 15 September 2022 from the GOPA reanalysis, which is representative of typical recirculations at these locations.



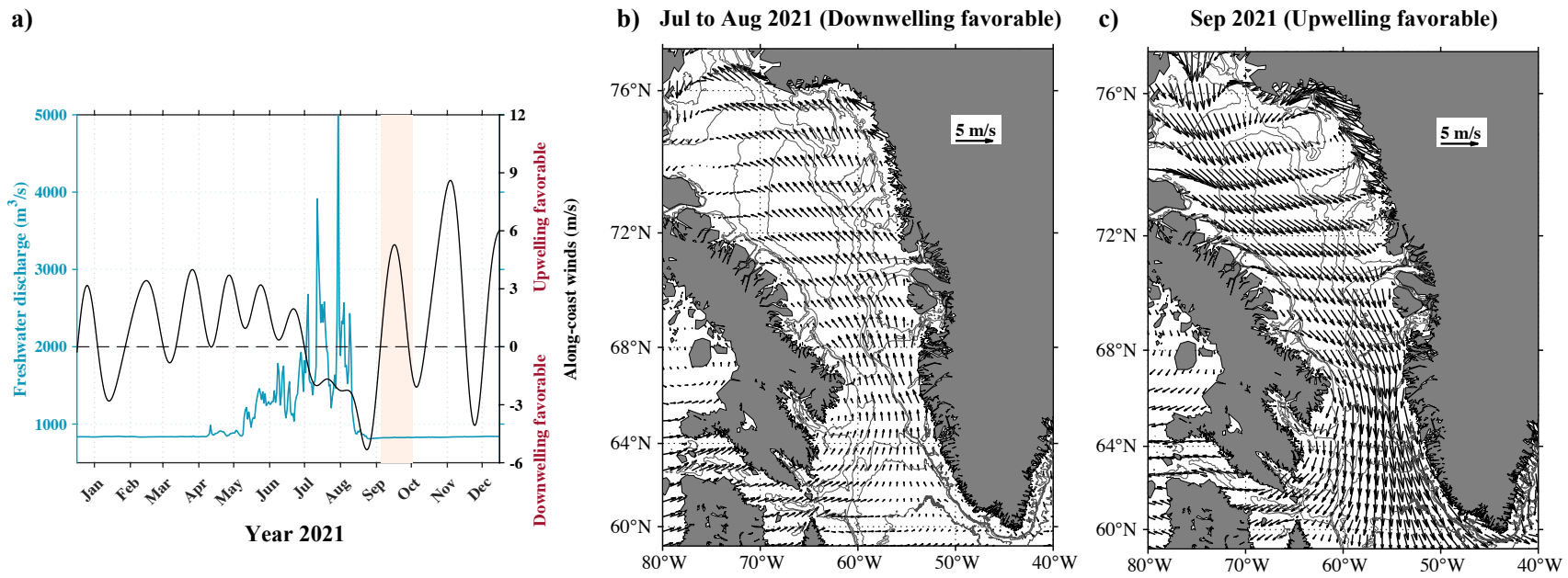
Supplementary Figure 1. Comparison of vertical sections of salinity and velocity (cm/s) for the two Uummannaq sections from the shipboard observations (left) and the GOPA reanalysis (right) over the same time period. Gray contours in the salinity panels indicate potential density (kg/m^3). In the velocity panel, black contours denote zero velocity; positive velocities are directed toward the glacial fjords.



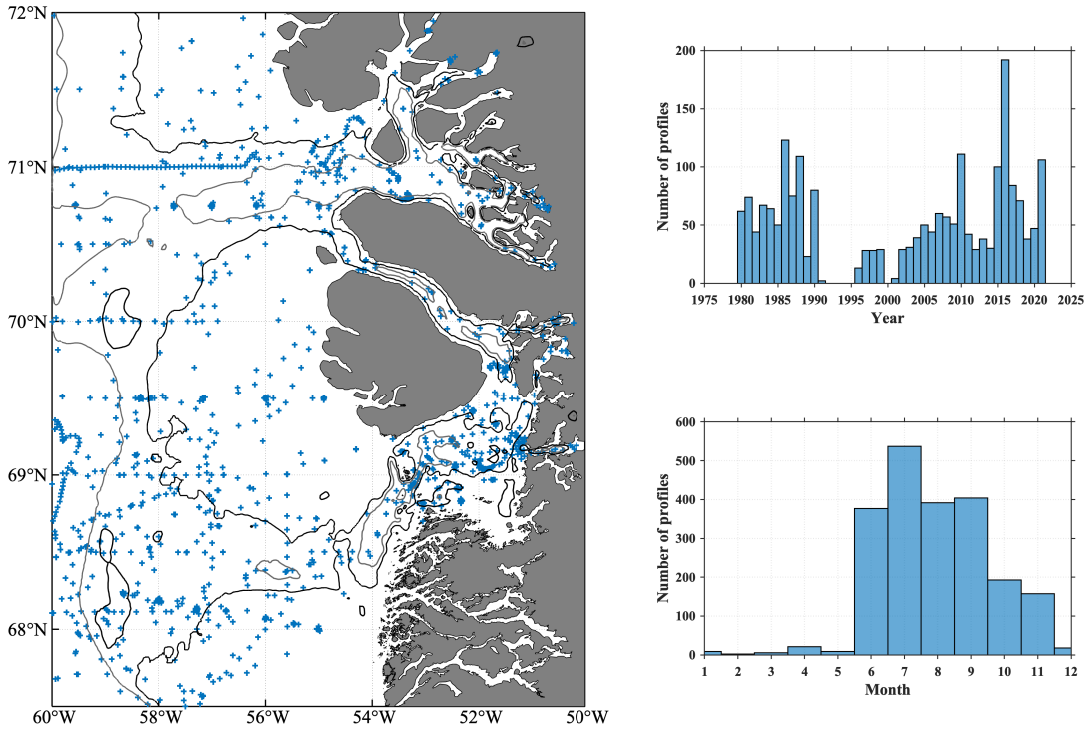
507

508

509 **Supplementary Figure 2.** (a) Timeseries of volume transport for the northern (blue) and southern
510 (red) halves of the inner Uummannaq section from the 1/60° model output. Pink shading denotes
511 periods of flow reversal from May to October when transport is reversed for roughly four weeks;
512 five such events are identified. (b) Composite depth-integrated volume transport for the five
513 reversal events as a function of normalized time. Shading indicates the standard error. (c-f)
514 Composite vertical sections of salinity and velocity for the outer (U2) and inner (U1) Uummannaq
515 sections during the peak of the events (normalized time 0.4-0.6). Gray contours in the salinity
516 panels indicate potential density (kg/m^3). In the velocity panel, black contours denote zero velocity;
517 positive velocities are directed toward the glacial fjords.



Supplementary Figure 3. (a) Timeseries of total freshwater discharge and alongcoast winds in the Uummannaq area during 2021. Positive values indicate upwelling favorable (northerly) winds and negative values indicate downwelling favorable (southerly) winds. Pink shading indicates the time period of the flow reversal identified from the GOPA reanalysis (event G1 in Fig. 4). (b) Mean wind vectors for July to August 2021 (downwelling favorable). (b) Wind vectors for September 2021 (upwelling favorable).



Supplementary Figure 4. Spatial (left) and temporal (right) coverage of the compiled historical hydrographic data near the Uummannaq and Jakobshavn areas. See Data Availability Section for the different data sources.